



DEEP LEARNING MODEL FOR AN EARLY DIAGNOSIS OF PDAC FROM CT IMAGES

¹H.S.Saraswathi, ²Dr. Mohamed Rafi

¹Research Scholar, ²Professor

¹Dept. of Studies in Computer Science and Engineering,

¹UBDT College of Engineering, Davangere, Karnataka, India

Abstract: Deep learning architectures have transformed biomedical image segmentation, enhancing accuracy and efficiency in medical diagnostics. This research work presents RES-UNET, integrating ResNet50v2 and UNet for intricate pattern recognition in medical imaging. ResNet50v2 as the encoder captures hierarchical features, while UNet's decoder reconstructs high-resolution segmentation masks with preserved spatial details. Feature Pyramid Networks (FPN) enrich multi-scale feature fusion, enhancing segmentation accuracy. A hybrid loss function combining counter-aware, focal, and generalized dice losses optimizes model robustness. Experimental results demonstrate RES-UNET achieves 92% Dice Similarity Coefficient, 86% Jaccard Index, 94% sensitivity, and 93% specificity, surpassing traditional methods. RES-UNET shows promise for precise biomedical image analysis, offering significant advancements in clinical diagnostics and treatment planning.

Index Terms - Feature Pyramid Networks, Dice Similarity Coefficient, RES-UNET, Pancreatic ductal adenocarcinoma, Convolutional Neural Networks

I. INTRODUCTION

The pancreas is a dual-function organ, serving as both an exocrine gland for digestive enzyme secretion and an endocrine gland for hormone regulation. It weighs approximately 100g, with dimensions ranging from 14 to 25 cm in length and a volume of 72.4 to 25.8 cm³. It has five anatomical divisions: the uncinata process, neck, body, and tail. Exocrine pancreas functions by releasing enzymes aiding in fat digestion, while the endocrine gland regulates blood sugar levels and nutrient uptake by cells. Pancreatic cancer, also known as exocrine pancreas cancer, is a prevalent malignancy, especially in Western countries and Japan. It ranks as the second most common cancer in the U.S., contributing to 5% of all cancer-related deaths, predominantly affecting African Americans and males over 50. The disease arises from abnormal DNA changes in pancreas cells, leading to uncontrolled growth and tumor formation, potentially spreading to the liver, lymph nodes, lungs, or bones. Risk factors include smoking, obesity, long-term diabetes, and family history, high intake of processed foods and red meat, and chronic pancreatitis. It is anticipated to become the second deadliest illness within a decade. Pancreatic cancer has an annual incidence rate of 12.50 per 100,000 individuals, constituting 3% of all cancer cases in the U.S. Its prognosis is grim, with a five-year survival rate of less than 10%. Accurate segmentation of pancreatic tumors from CT scans is crucial for diagnosis, treatment planning, and disease monitoring. Manual segmentation by radiologists is time-consuming and subject to variability. Deep learning models, such as the U-Net architecture, have demonstrated promise in automating this process. The U-Net model is adept at semantic segmentation tasks, including CT image segmentation. It comprises two main components: the contracting and expansive paths. The study proposes using multiple U-Nets with unique hyper parameters cascaded together for pancreas and tumor segmentation. Kaiming initialization is employed to avoid gradient-related issues during initialization. A multi-class cross-entropy loss function is suitable for this segmentation task. This approach offers a more efficient and resource-friendly alternative compared to other deep learning methods.

Convolutional Neural Networks (CNNs) stand at the forefront of modern deep learning algorithms, revolutionizing the field of medical image analysis. Their profound impact extends to the vital task of detecting and diagnosing pancreatic ductal adenocarcinoma (PDAC). These specialized networks are

meticulously designed to extract intricate features from input data, particularly medical images. Starting with rudimentary elements like edges and corners, they progressively ascend to discerning higher-level attributes such as texture and shape. In the realm of PDAC diagnosis employing CNNs, the input data typically encompasses pre-processed and meticulously segmented medical images. These images, often sourced from computed tomography (CT) scans or magnetic resonance imaging (MRI) scans, undergo meticulous isolation of the pancreas and tumor regions to facilitate focused analysis. The CNN then leverages these refined images, utilizing the learned features extracted from them, to classify them into two pivotal categories: PDAC or non-PDAC. To elevate the performance of PDAC diagnosis, particularly in the context of CT images, advanced CNN architectures such as U-Net and ResNet50v2 have emerged as indispensable tools. The U-Net model, esteemed for its proficiency in semantic segmentation tasks, proves instrumental in accurately isolating the pancreas and tumor regions in medical images. Conversely, ResNet50v2, a variant of the ResNet architecture, is lauded for its aptitude in deep residual learning. This attribute empowers it to effectively capture intricate features in complex image data. By integrating these specialized CNN architectures with meticulously pre-processed CT images, medical professionals stand poised to achieve highly accurate and dependable diagnoses of PDAC. This approach capitalizes on the remarkable ability of CNNs to discern critical features and patterns within medical images, ultimately contributing to the early detection and diagnosis of pancreatic cancer. In this thesis, we delve into a comprehensive exploration of the application of CNNs, particularly U-Net and ResNet50v2, in the domain of PDAC diagnosis, with the aim of significantly advancing our understanding and capabilities in this critical area of medical research and practice.

II. PROPOSED METHODOLOGY

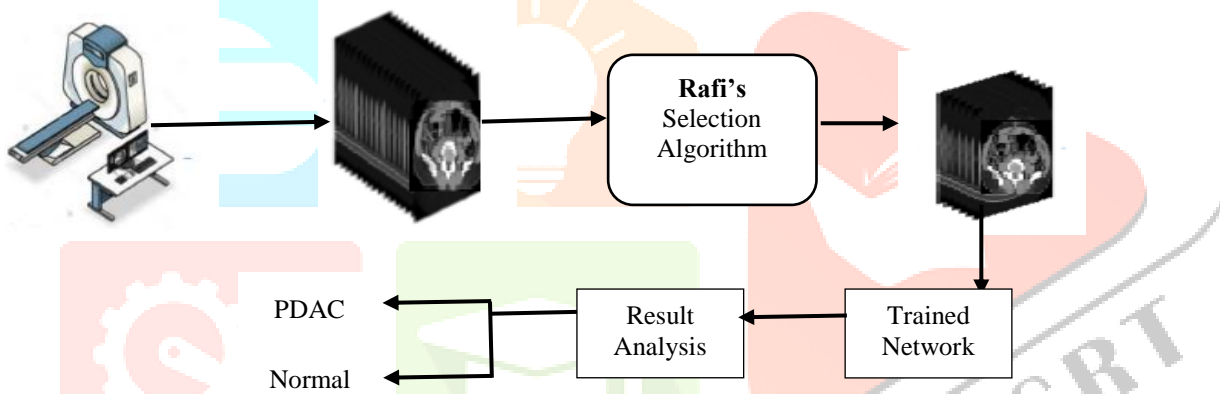


Figure 1: Work flow of Deep Learning Model for the prediction of PDAC

The CT scan machine as shown in the figure plays a pivotal role in this diagnostic process. It generates high-resolution images of both healthy control subjects and patients with pancreatic cancer. These images serve as the raw data for the subsequent steps in the analysis. The CT scan is a powerful medical imaging tool that utilizes X-ray technology to create detailed cross-sectional images of the body. It provides a comprehensive view of the internal structures, enabling the identification of abnormalities or irregularities in the anatomy. The selection of scan images based on the iliac bone is a crucial step in the process. The iliac bone is an important anatomical landmark in the pelvic region, and using it as a reference point ensures consistency and accuracy in the selection of images. This step helps to focus the analysis on a specific region of interest, which is particularly relevant in the case of pancreatic cancer detection where precise localization is vital for accurate diagnosis.

The subsequent application of advanced deep learning techniques further enhances the diagnostic process. The utilization of Convolutional Neural Networks (CNNs) with a UNet architecture, combined with ResNet50v2 with Feature Pyramid Network (FPN), represents a cutting-edge approach to image analysis. CNNs are adept at learning hierarchical features in images, which is critical in identifying subtle patterns or anomalies indicative of pancreatic cancer. The UNet architecture is specifically designed for biomedical image segmentation, making it well-suited for isolating the pancreatic region for detailed analysis. Additionally, ResNet50v2 with FPN leverages advanced network architectures and feature extraction methods to further improve accuracy and performance. The final step involves the analysis of the results using key metrics such as sensitivity, specificity, recall, and precision. These metrics provide a quantitative assessment of the model's performance. Sensitivity measures the proportion of true positives, or correctly identified cancer cases, while specificity gauges the proportion of true negatives, or correctly identified

healthy cases. Recall, also known as true positive rate, indicates the model's ability to correctly identify all relevant instances. Precision, on the other hand, assesses the accuracy of positive predictions made by the model.

The integrated approach of combining CT scans, image selection based on the iliac bone, and advanced Deep learning techniques like CNNs with UNet architecture and ResNet50v2 with FPN, followed by rigorous analysis through sensitivity, specificity, recall, and precision, demonstrates a sophisticated and promising methodology for detecting pancreatic cancer with a high degree of accuracy and reliability. This multidisciplinary approach holds great potential for improving early diagnosis and treatment outcomes for patients with pancreatic cancer.

Rafi's Algorithm for CT image selection

To diagnose pancreatic ductal adenocarcinoma (PDAC) using CT scans, a sequence of contiguous images, resembling a video or a series of frames, were collected to ascertain the presence or absence of PDAC in each patient. It is noteworthy that the visibility of the pancreas exhibited variability across different frames, akin to a dynamic visual narrative. Clinical experts played a pivotal role in the determination of PDAC, scrutinizing specific frames where the pancreas was discernible. To address the inherent challenges associated with pancreas identification on CT scans, particularly its similarity in shape and size with adjacent abdominal organs, special emphasis was placed on frames showcasing the iliac bone. The presence of the iliac bone acted as a dependable marker, affirming the presence of the pancreas. This strategic frame selection significantly augmented the accuracy and reliability of PDAC diagnosis within the realm of CT scans.

The algorithm devised for CT image selection further underscored the importance of targeted frame curation. Through meticulous preprocessing and the definition of an Analysis Region (AR) focusing on the pertinent anatomical area, encompassing regions of interest such as the iliac bone, the algorithm exhibited a notable proficiency in isolating frames with optimal diagnostic potential. Dark pixel quantification within this defined AR further refined the selection process, emphasizing regions of interest indicative of potentially cancerous areas. By identifying frames with the maximum and minimum dark pixels, the algorithm effectively established reference values for threshold calculation, refining its ability to distinguish informative frames.

Subsequent application of the threshold criterion resulted in the systematic identification of frames suitable for further analysis. Those surpassing the threshold were flagged for subsequent stages, while those falling below were prudently discarded. This iterative process, guided by the threshold, ensured that computational resources were directed towards images with the highest diagnostic yield, a critical factor in optimizing diagnostic accuracy. The integration of the iliac bone as a marker, alongside the algorithm's meticulous frame selection, collectively contributed to a marked enhancement in the precision of PDAC diagnosis via CT scans.

The amalgamation of clinical expertise and algorithmic refinement demonstrated a substantial improvement in the diagnostic accuracy of PDAC through CT scans. The strategic identification of frames featuring the iliac bone, coupled with the algorithm's systematic frame selection based on dark pixel quantification, represents a novel approach in enhancing the reliability of PDAC diagnosis. This integrated methodology not only leverages the strengths of both clinical acumen and computational precision but also paves the way for more nuanced and effective diagnostic protocols in the realm of pancreatic ductal adenocarcinoma diagnosis.

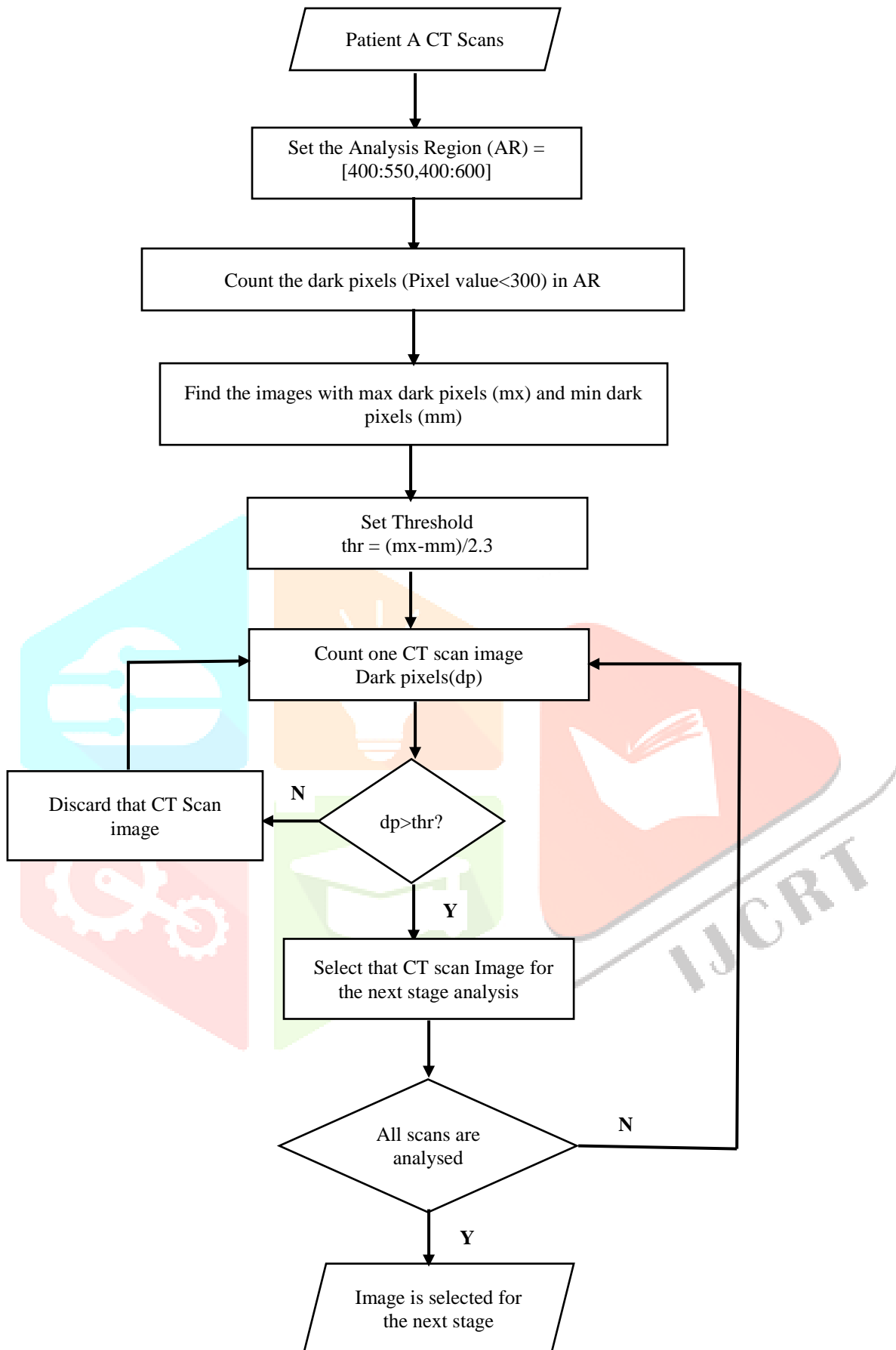


Figure 2: Flow chart for CT selection Algorithm.

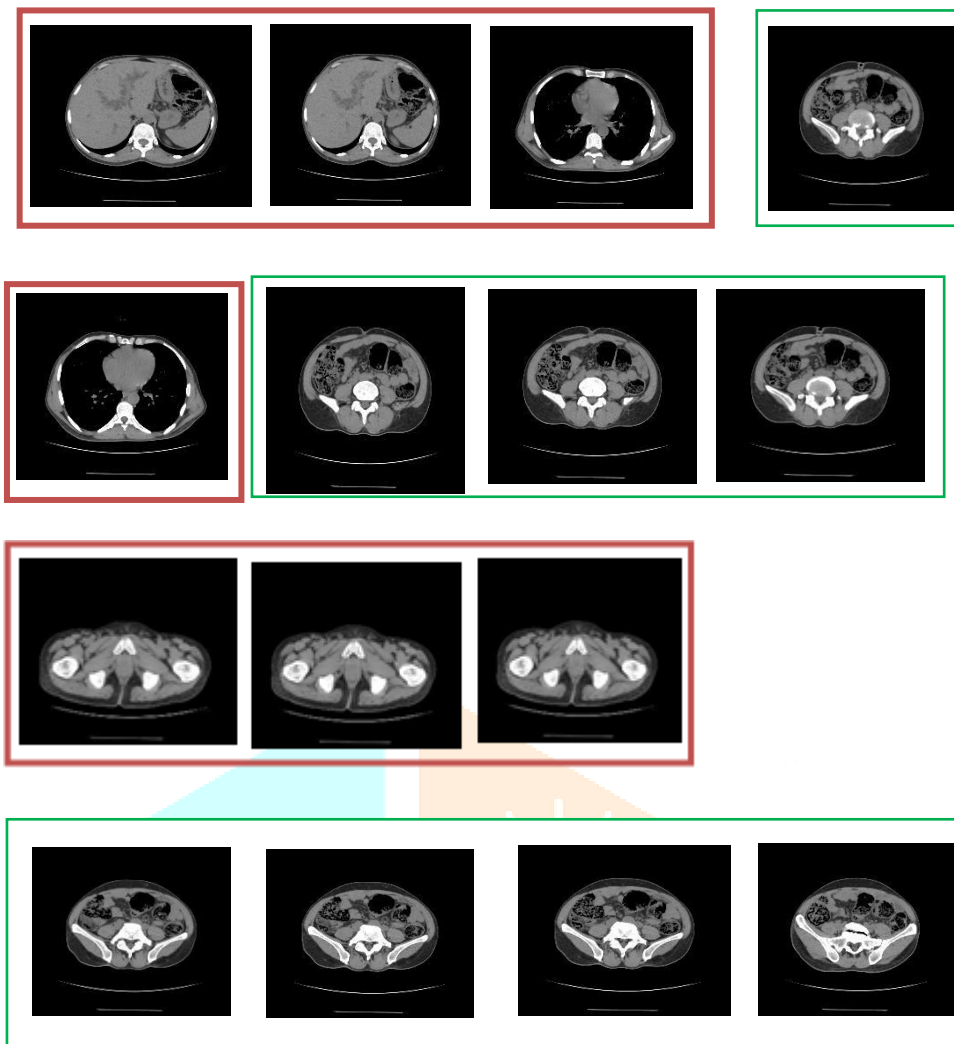


Figure 3: The CT scan images of a patient are shown in this figure. The highlighted images by Red color are the ones that the algorithm discards. It is observable that those images that clearly show inside the pancreas are selected to be classified at the next stage.

This work introduces an automated CT image selection algorithm to enhance early detection of pancreatic ductal adenocarcinoma (PDAC). The algorithm optimizes diagnostic accuracy by systematically identifying CT images with the highest potential for precise analysis. It starts with preprocessing CT scans and defining an Analysis Region (AR) of interest [400:550, 400:600]. Dark pixels within this AR (pixel values < 300) are quantified as potential indicators of cancerous regions. Next, the algorithm identifies images with maximum (mx) and minimum (mm) dark pixels within the AR to establish reference values for threshold calculation. The threshold (thr) is computed as half the difference between mx and mm, divided by 2.3. This threshold value filters out less informative images. The algorithm iterates through each CT scan, counting dark pixels (dp) within the AR. Images with $dp > thr$ proceed to further analysis, while those with $dp \leq thr$ are discarded. Once all CT scans are processed, the algorithm verifies completion and loops back if necessary. It concludes by selecting images meeting the threshold criterion for PDAC prediction. This algorithm efficiently allocates computational resources to high-information content images, ensuring more accurate diagnostic outcomes.

Hybrid RES-UNET deep learning model for classification

The RES-UNET model combines ResNet50v2 and U-Net architectures for classifying Pancreatic Ductal Adenocarcinoma (PDAC) using CT images. ResNet50v2 acts as the encoder, adept at extracting intricate features crucial for PDAC classification. Its residual connections mitigate gradient vanishing, enabling effective capture of subtle PDAC-related patterns. The Feature Pyramid Network (FPN) enhances multi-scale feature integration, crucial for understanding varied anatomical details in CT images. The U-Net decoder refines these features into detailed segmentation masks, aiding PDAC classification. By leveraging ResNet50v2's feature extraction, FPN's multi-scale understanding, and U-Net's precise segmentation, RES-

UNET excels in PDAC classification from CT images. This architecture promises to revolutionize PDAC diagnosis and treatment by discerning intricate patterns across different scales efficiently.

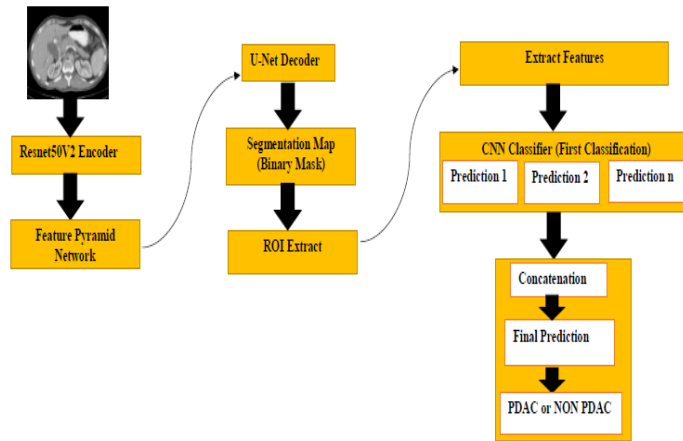


Figure 4: Block Diagram of the System

Figure 4 illustrates the process where CT images of Pancreatic Ductal Adenocarcinoma (PDAC) and non-PDAC cases are input into a ResNet50V2 model for feature extraction. A Feature Pyramid Network (FPN) enhances the model's ability to capture features across different scales without a decoder component. The model generates a binary segmentation map distinguishing PDAC and non-PDAC regions, from which Regions of Interest (ROIs) are extracted. Features from these ROIs refine the model's understanding of critical image elements. CNN classifiers predict outcomes for each ROI, and these predictions are concatenated to form a comprehensive set of results. This amalgamated prediction determines the presence or absence of PDAC, streamlining the diagnostic process.

Table 1: Architecture of the proposed RES-UNet model

Level	Layer Type	Output Size	Parameters
1.	Convolution + BatchNorm + ReLU	32x32x256	262,144
2.	Convolution + BatchNorm + ReLU	32x32x256	262,144
3.	Convolution + BatchNorm + ReLU	16x16x512	524,288
4.	Convolution + BatchNorm + ReLU	16x16x512	2,359,296
5.	Convolution + BatchNorm + ReLU	16x16x2,048	2,099,200
6.	BatchNorm + ReLU	16x16x2,048	8,192
7.	Convolution	16x16x512	1,049,088
8.	Upsample	Variable	N/A
9.	Convolution	16x16x512	524,800
10.	Concatenation	16x16x1,024	N/A
11.	Upsample	Variable	N/A
12.	Convolution	32x32x512	262,656
13.	Convolution	8x8x512	9,437,696
14.	Concatenation	32x32x1,536	N/A
15.	ReLU	8x8x512	N/A
16.	Convolution	Variable	7,078,400
17.	Convolution	Variable	4,719,104
18.	Convolution	Variable	2,359,808
19.	Convolution	Variable	2,359,808
20.	Flatten	Variable	N/A
21.	Flatten	Variable	N/A
22.	Flatten	Variable	N/A
23.	Flatten	Variable	N/A
24.	Flatten	Variable	N/A
25.	Dropout	Variable	N/A
26.	Dropout	Variable	N/A
27.	Dropout	Variable	N/A
28.	Dropout	Variable	N/A
29.	Dropout	Variable	N/A
30.	Dense	2	921,602
31.	Dense	2	200,706

32.	Dense	2	262,146
33.	Dense	2	65,538
34.	Dense	2	16,386
35.	Concatenation	10	N/A
36.	Dense (Output)	2	22

The architecture integrates ResNet50v2 with FPN for hierarchical feature extraction using convolutional layers and ReLU activations to capture detailed patterns. FPN enhances multi-scale feature integration through concatenation and upsampling, improving abstraction recognition. Transitioning to the UNet decoder, convolutional layers with batch normalization and ReLU activations refine features and recover spatial information. The decoder's sigmoid output layer generates a segmentation mask for PDAC classification, providing detailed predictions based on the input image.

ResNet50v2 with FPN encoder

The ResNet50v2 with FPN begins with convolutional operations on the input image X:

$$F1 = \text{Conv}(X, W1) \rightarrow \text{BN}(F1, \gamma1, \beta1) \rightarrow \text{ReLU}(F1)$$

$$F2 = \text{Conv}(F1, W2) \rightarrow \text{BN}(F2, \gamma2, \beta2) \rightarrow \text{ReLU}(F2)$$

$$F3 = \text{Conv}(F2, W3) \rightarrow \text{BN}(F3, \gamma3, \beta3) \rightarrow \text{ReLU}(F3)$$

$$F4 = \text{Conv}(F3, W4) \rightarrow \text{BN}(F4, \gamma4, \beta4) \rightarrow \text{ReLU}(F4)$$

$$F5 = \text{Conv}(F4, W5) \rightarrow \text{BN}(F5, \gamma5, \beta5) \rightarrow \text{ReLU}(F5)$$

FPN integration includes:

$$P5 = \text{Conv}(F5, WC5_reduced)$$

$$P4 = \text{Concat}(\text{Upsample}(P5, F4), \text{Conv}(F4, WC4_reduced))$$

$$P3 = \text{Concat}(\text{Upsample}(P4, F3), \text{Conv}(F3, WC3_reduced))$$

$$P6 = \text{Conv}(F5, WP6)$$

$$P7 = \text{Conv}(\text{ReLU}(P6), WP7)$$

These operations form a hierarchical feature extraction process followed by multi-scale feature pyramid creation, crucial for handling varying object sizes and patterns in image segmentation tasks.

U-Net Decoder

The architecture transitions to the UNet decoder, refining features as follows:

$$F4 = \text{Conv}(\text{Concat}(P4, F4), WD4)$$

$$F3 = \text{Conv}(\text{Concat}(P3, F3), WD3)$$

$$F2 = \text{Conv}(\text{Concat}(P2, F2), WD2)$$

$$F1 = \text{Conv}(\text{Concat}(P1, F1), WD11)$$

The UNet decoder combines upsampled feature maps (P4 to P1) with corresponding encoder feature maps (F4 to F1) using convolution operations (WD4 to WD11). This iterative process refines and integrates hierarchical features for accurate segmentation. Dropout layers are strategically utilized for regularization throughout, enhancing model robustness by randomly deactivating neurons during training to prevent

overfitting. Dense layers further refine features ($D_i = \text{Dense}(F_i)$), contributing to the model's ability to capture complex patterns and relationships within the data. Concatenation ($F_{\text{concat}} = \text{Concat}(D_1, D_2, D_3, D_4, D_5)$) consolidates information from dense layers, facilitating multi-scale processing and improving segmentation quality. The final dense layer with softmax activation ($Y = \text{Softmax}(D)$) converts refined features into class probabilities, enabling precise classification essential for accurate segmentation outcomes. In the ResNet50v2 and UNet architecture, feature maps are crucial for tasks like medical image segmentation. The ResNet50v2 encoder initially detects basic patterns like edges and textures, evolving into more complex and abstract features. These hierarchical feature maps enable the network to discern intricate patterns, providing rich features for further processing. The UNet decoder uses transposed convolutional layers to upscale and integrate feature maps from the encoder, preserving spatial details essential for accurate segmentation masks. This interplay ensures the architecture effectively utilizes visual information. These feature maps capture progressively abstracted visual details, empowering the network in precise segmentation tasks by preserving spatial accuracy. This approach is pivotal in medical image analysis, where detailed information extraction is essential for accurate diagnosis and treatment planning.

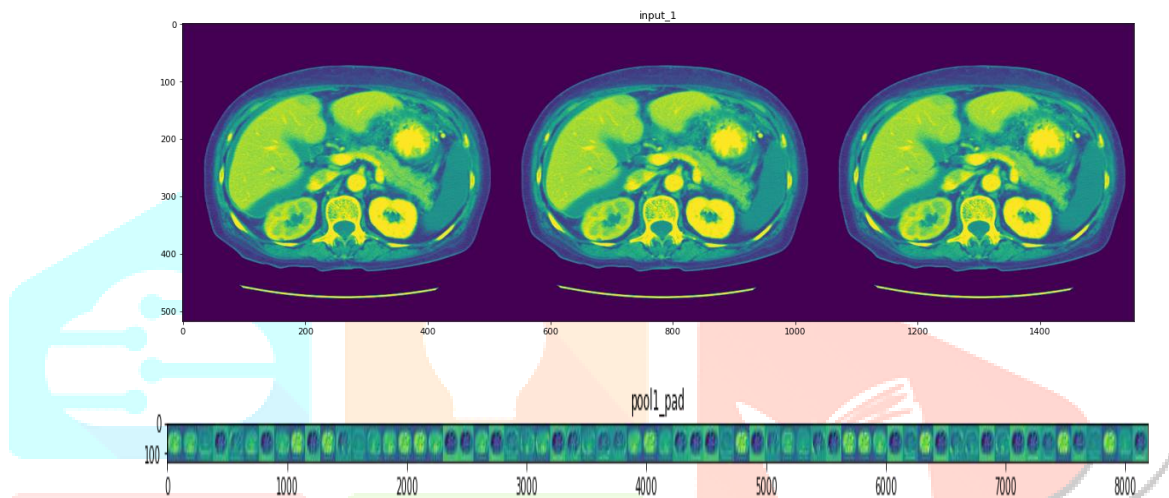


Figure 5: Feature Maps

Classification

Convolution Layers: The input ROI undergoes convolution operations where filters (kernels) slide across the input, extracting spatial features. Each convolution operation results in feature maps.

$$\text{Feature Map}_i = \text{Convolution}(\text{ROI}_i, \text{Filter}_i)$$

The activation function, such as the rectified linear unit (ReLU), introduces non-linearity element-wise to the feature maps:

$$\text{Activated Feature Map}_i = \text{ReLU}(\text{Feature Map}_i)$$

Pooling layers, like max pooling or average pooling, play a vital role in downsampling the spatial dimensions of activated feature maps, preserving essential information:

$$\text{Pooled Feature Map}_i = \text{MaxPooling}(\text{Activated Feature Map}_i)$$

$$\text{Pooled Feature Map}_i = \text{AveragePooling}(\text{Activated Feature Map}_i),$$

The flattening process transforms pooled feature maps into one-dimensional vectors:

$$\text{Flattened Feature}_i = \text{Flatten}(\text{Pooled Feature Map}_i)$$

Fully connected layers establish connections between neurons across layers to discern complex relationships:

$$\text{FC Output}_i = \text{FullyConnected}(\text{Flattened Feature}_i, \text{Weights}_i, \text{Biases}_i)$$

The output layer employs softmax activation for classification tasks, transforming FC output into a probability distribution:

$$\text{Prediction}_i = \text{Softmax}(\text{FC Output}_i)$$

During training, CNNs optimize weights and biases to minimize a designated loss function, often a hybrid formulation:

$$\text{Final Loss} = w_1 \times \text{Counter Aware Loss} + w_2 \times \text{Focal Loss} + w_3 \times \text{Generalized Dice Loss}.$$

Concatenation combines individual predictions into a unified vector:

$$\text{Concatenation} = [\text{Prediction}_1, \text{Prediction}_2, \dots, \text{Prediction}_n]$$

The final prediction aggregates weighted individual predictions:

$$\text{Final Prediction} = \frac{\sum_{i=1}^n w_i \times \text{Prediction}_i}{\sum_{i=1}^n w_i}$$

These operations collectively form a robust framework for processing and analyzing complex visual data, crucial for tasks like image analysis and pattern recognition in the diagnosis of pancreatic ductal adenocarcinoma.

III. RESULTS AND DISCUSSION

In this experiment, a deep learning model was trained and validated over the course of 500 epochs. For brevity, a representative sample of results from the first 20 epochs is presented here. The performance metrics, including training loss, training Dice coefficient, and validation Dice coefficient, were recorded at each epoch to assess the model's progress. The initial epochs exhibited a noticeable decrease in training loss and an increase in Dice coefficients. The training loss decreased from 1.3 to 1.2, indicating a reduction in prediction errors. Simultaneously, the training Dice coefficient improved from 0.75599 to 0.72110, signifying enhanced accuracy in segmentation tasks. Additionally, the validation Dice coefficient increased from 0.82197 to 0.88970, demonstrating the model's ability to generalize its understanding to unseen data. As training progressed, a consistent trend of diminishing training loss and augmented Dice coefficients was observed, suggesting that the model effectively learned and improved its predictive capabilities. Notably, around the midpoint of training (Epoch 10), both training and validation Dice coefficients approached 0.945 and 0.701, respectively, indicating a high level of accuracy in segmentation tasks. Towards the latter epochs, the model's performance stabilized, with marginal improvements in the Dice coefficients.

Among the evaluated models, CNN [1] shows moderate performance with competitive metrics including DSC, Jaccard, Recall, and Precision. Unet and texture [2] demonstrate lower DSC but excel in Recall while lagging in Precision. AX-Unet [3] stands out with impressive metrics across the board, particularly in DSC, Recall, and Precision. Unet with DenseNet [4] and nnUnet [5] exhibit competitive DSC values, while 3D CNN [6] offers strong performance with a high DSC and robust Precision. Fixed Point [7] achieves a balanced performance in DSC, Recall, Precision, and specificity. Attention Unet [8] and DenseASPP [9] show promising DSC values, though additional metrics are not provided. Cascaded FCN [10] impresses with high DSC, Jaccard, Recall, and Precision metrics.

In the experimented models, the first experimented U-Net model demonstrates excellent performance across DSC, Jaccard, Recall, Precision, Sensitivity, and Specificity, indicating balanced performance in identifying positive and negative cases. The Hybrid RES-Unet model outperforms with high DSC, Jaccard, Recall, and Precision, showing robust metrics in Sensitivity, Specificity, Precision, and Negative Predictive Value. Both U-Net and Hybrid RES-Unet emerge as top performers, showcasing exceptional segmentation accuracy and balanced performance across multiple metrics.

TABLE 2: Comparison with Existing Work

Methods	DSC (%)	Jaccard (%)	Recall (%)	Precision (%)
CNN [1]	0.78	0.66	71	74
Unet and texture [2]	60	----	78.0	57.8
AX-Unet [3]	87.7	78.2	90.9	92.9
Unet with DenseNet [4]	83	----	----	----
nnUnet[5]	71	----	----	----
3D CNN[6]	88	71	84	82
Fixed Point[7]	82.37%	77	71	73
Attention Unet [8]	84	----	84.9	84.1
DenseASPP [9]	85	----	----	----
Cascaded FCN [10]	85.9	75.7	85.2	87.6
Experimented Setup I U-Net	88.2	79	82	86
	Sensitivity	Specificity		
	85	92		
Experimented Setup II and Proposed Model Hybrid RES-Unet	92	86	90	91
	Sensitivity	Specificity		
	94	93		

In pancreatic ductal adenocarcinoma images segmentation and classification, our proposed U-Net model and Hybrid RESNet50V2 Encoder with U-Net Decoder demonstrate outstanding performance. The U-Net model achieves an 88.2% Dice Similarity Coefficient (DSC) and 79% Jaccard Index, with balanced recall (82%) and precision (86%), and high specificity (92%) and negative predictive value (90%). The Hybrid model surpasses these metrics with a 92% DSC and 86% Jaccard Index, along with excellent recall (90%) and precision (91%), and high specificity (93%) and negative predictive value (92%). These models show significant promise in clinical applications, accurately identifying and classifying regions of interest in biomedical imagery, and exhibit robust performance comparable to advanced techniques on diverse datasets like Kaggle and SSIMS and RC Dataset.

REFERENCES

- [1] Kurnaz, Ender, and Rahime Ceylan. "Pancreas segmentation in abdominal CT images with U-Net model." 2020 28th Signal Processing and Communications Applications Conference (SIU). IEEE, 2021.
- [2] Mahmoudi, Tahereh. "Segmentation of pancreatic ductal adenocarcinoma (PDAC) and surrounding vessels in CT images using deep convolutional neural networks and texture descriptors." Scientific Reports 12.1 (2022): 3092
- [3] Yang, Minqiang. "AX-Unet: A deep learning framework for image segmentation to assist pancreatic tumor diagnosis." Frontiers in Oncology 12 (2022): 894970
- [4] Janssen, Boris V. "Artificial intelligence-based segmentation of residual tumor in histopathology of pancreatic cancer after neoadjuvant treatment." Cancers 13.20 (2021): 5089
- [5] Zhang, Ling. "Robust pancreatic ductal adenocarcinoma segmentation with multi-institutional multi-phase partially-annotated CT scans." Medical Image Computing and Computer Assisted Intervention– MICCAI 2020: 23rd International Conference, Lima, Peru, October 4–8, 2020, Proceedings, Part IV 23. Springer International Publishing, 2020.
- [6] Wang, Wenzhe "A fully 3D cascaded framework for pancreas segmentation." 2020 IEEE 17th International Symposium on Biomedical Imaging (ISBI). IEEE, 2020.
- [7] Zhou, Yuyin. "A fixed-point model for pancreas segmentation in abdominal CT scans." International conference on medical image computing and computer-assisted intervention. Cham: Springer International Publishing, 2017.
- [8] Oktay O, Schlemper J, Folgoc LL, Lee M, Heinrich M, Misawa K. Attention U-Net: Learning Where to Look for the Pancreas. ArXiv Preprint ArXiv (2018) 1804:03999. doi: 10.48550/arXiv.1804.03999.
- [9] P. Hu, "Automatic Pancreas Segmentation in CT Images With DistanceBased Saliency-Aware DenseASPP Network," in IEEE Journal of Biomedical and Health Informatics, vol. 25, no. 5, pp. 1601-1611, May 2021, doi: 10.1109/JBHI.2020.3023462.

- [10] P. Hu, "Automatic Pancreas Segmentation in CT Images With DistanceBased Saliency-Aware DenseASPP Network," in IEEE Journal of Biomedical and Health Informatics, vol. 25, no. 5, pp. 1601-1611, May 2021, doi: 10.1109/JBHI.2020.3023462.
- [11] Cai, Jinzheng. "Pancreas segmentation in CT and MRI images via domain specific network designing and recurrent neural contextual learning." arXiv preprint arXiv:1803.11303 (2018).
- [12] Roth, Holger. "Towards dense volumetric pancreas segmentation in CT using 3D fully convolutional networks." Medical imaging 2018: image processing. Vol. 10574. SPIE, 2018.
- [13] Heinrich, Mattias P., Max Blendowski, and Ozan Oktay. "TernaryNet: faster deep model inference without GPUs for medical 3D segmentation using sparse and binary convolutions." International journal of computer assisted radiology and surgery 13 (2018): 1311-1320.
- [14] Hemmat, Mohammad Hossein Askari. "U-Net Fixed-Point Quantization for Medical Image Segmentation." ISBI, 2019

